ASSESSMENT OF THERMAL LOADS IN THE CERN SPS CRAB CAVITIES CRYOMODULE*

F. Carra†, J. Apeland, R. Calaga, O. Capatina, T. Capelli, C. Zanoni, CERN, Geneva, Switzerland
S. Verdú-Andrés, BNL, Upton, NY 11973, USA

Abstract

As a part of the HL-LHC upgrade, a cryomodule is designed to host two crab cavities for a first test with protons in the SPS machine.

The evaluation of the cryomodule heat loads is essential to dimension the cryogenic infrastructure of the system. The current design features two cryogenic circuits. The first circuit adopts superfluid helium at 2 K to maintain the cavities in the superconducting state. The second circuit, based on helium gas at a temperature between 50 K and 70 K, is connected to the thermal screen, also serving as heat intercept for all the interfaces between the cold mass and the external environment. An overview of the heat loads to both circuits, and the combined numerical and analytical estimations, is presented. The heat load of each element is detailed for the static and dynamic scenarios, with considerations on the design choices for the thermal optimization of the most critical components.

INTRODUCTION AND HEAT BUDGET

One key element of the next LHC upgrade, known as HL-LHC, is represented by the adoption of a crab-crossing scheme, provided by a set of compact SRF crab cavities [1]. Prior to installation in the LHC, a prototype two-cavity cryomodule was designed and is under manufacturing, in view of beam tests in the SPS in 2018 [2, 3].

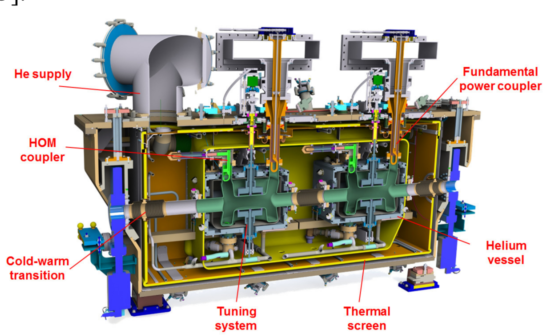

Figure 1: Cavity and interfaces.

The cavities are cooled with superfluid helium at 2 K, and a second circuit with helium gas, at a temperature between 50 K and 70 K, is connected to the thermal screen, also serving as heat intercept for all the elements connecting the cold mass and the external environment. Detailed calculations were performed in order to evaluate the thermal losses to the two cooling circuits, a necessary input for the design of the cryogenic infrastructures. The thermal losses breakdown is shown in Table 1, referring to both circuits in static (without RF power) and dynamic (with RF power, cavity delivering 3.4 MV deflecting voltage) nominal HL-LHC working conditions. The main items contributing to the total losses and the thermal design choices are summarized in the next sections. While the He gas circuit is at a temperature comprised between 50 K and 70 K, the connection to the intercepted components is done by means of copper flexures at a temperature conservatively assumed equal to 80 K.

Table 1: Cryomodule Heat Loads. Values are in Watts

	2 K	**80 K**
Static		
Radiation	3.4	30
Cold/Warm transitions	0.2	10
Supports	2	40
FPC	4	100
Instrumentation	2.3	10
HOM/Pickup	3.9	40
Tuner	1	10
Total static	**16.8**	**240**
Dynamic		
Cavity deflecting mode	11	0
FPC	5	10
HOM/Pickup	4.9	10
Beam current	0.5	0
Total Dynamic	**21.4**	**20**
TOTAL	**38.2**	**260**

SUPPORTS, TUNING SYSTEM AND COLD/WARM TRANSITIONS

These elements are not traversed by electrical currents and contribute therefore only to the static losses of the system. Their thermal design keeps into account the heat flowing by conduction from the thermal screen circuit to the helium tank (80 K – 2 K), and exchanged between the external ambient and the thermal screen (300 K – 80 K). The contribution of thermal radiation was also investigated and found to be negligible; therefore the problem is solved analytically, for each element, with the *Fourier's equation*:

$$Q_{2K} = \frac{A}{L_{int}} \int_{2K}^{80K} k(T)dT$$
$$Q_{80K} = \frac{A}{L - L_{int}} \int_{80K}^{300K} k(T)dT \quad (1)$$

*Work supported by the European Union HL-LHC Project and by US DOE through Brookhaven Science Associates LLC under contract No. DE-AC02-98CH10886 and the US LHC Accelerator Research Program (LARP). Research supported by the HL-LHC project.
† federico.carra@cern.ch

ISBN 978-3-95450-182-3

where k is the thermal conductivity, A and L are section and length of the connection, L_{int} is the distance between the cold mass and the intercept on the 80 K circuit. This is valid for geometries of constant thickness; for more complex shapes or 3D problems, the calculation was refined with a finite element analysis (FEA). Good thermal performances have to be reached without endangering the structural resistance of the component, and the technical solutions aim at the best thermal/mechanical compromise.

Supporting System

As shown in Figure 2, the dressed cavities are mechanically supported via the external tube Fundamental Power Coupler (FPC) and two 316LN blades [4]. The helium biphase line is supported on 316LN and Ti-6Al elements connected to the vacuum tank. All these components are quite massive; however, stainless steel and titanium are bad thermal conductors and the power losses to the cold mass, calculated with Eq. (1), are acceptable.

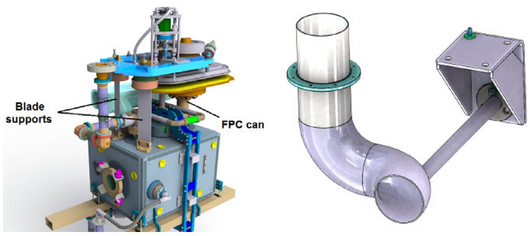

Figure 2: Left: cavity supports. Right: He line support.

Cold/warm Transitions (CWT)

The CWT are elements connecting the cavity to the warm beam line, and are constituted of a stainless steel beam pipe and bellows of the same material (see Figure 1). The system can be represented by two resistances in series, and since the bellows thickness is extremely low (0.15 mm), the thermal losses are negligible.

Tuning System

The tuner changes quasi symmetrically the distance between the two capacitive parts of the cavity. This is done by an actuator outside the cryostat that, acting on a titanium pushrod, creates a displacement between two vertical stainless steel concentric tubes [5].

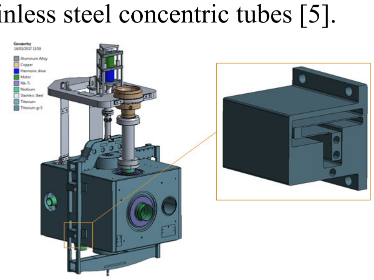

Figure 3: Left: tuning system. Right: detail of the connection frame/helium vessel.

The thermal losses to the cold mass are generated through the pushrod, the tubes and a rigid titanium frame surrounding the helium tank. The frame is in contact with the helium tank in four points, designed to maximize the thermal resistance while sustaining the mechanical stress given by the tuning actuation, avoiding the risks of buckling (Figure 3).

INSTRUMENTATION

The cryomodule is extensively instrumented, by means of temperature probes and magnetic flux sensors. Moreover, heaters are included at the end of each cold/warm line, at the vacuum tank level, to avoid the formation of ice (Figure 4). The wires for the powering of these systems act as resistances in parallel. Although each wire is very resistive, due to the high number of wires the total loss to the cold mass is quite relevant (above 2 W).

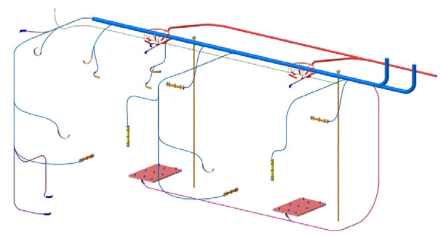

Figure 4: Wiring system. Different lines highlighted: thermal probes (purple), magnetic flux sensors (blue) and heaters (red).

THERMAL SCREEN

The thermal screen is a copper structure wrapped with multilayer insulation (MLI) and directly thermalized by the 80 K helium gas circuit (Figure 5). Its role is to minimise the thermal losses by radiation to the cold mass at 2 K [6]. In principle, the contribution of thermal radiation to the heat balance is not difficult to estimate for two grey bodies at a known emissivity by means of the *Stefan-Boltzmann law*. However, the addition of MLI complicates the problem, and the losses on the two circuits were estimated based on experimental measurements performed on LHC cryostats [7]. The thermal screen also presents openings required by the alignment instrumentation, allowing an optical access to the targets. At these openings, the cold mass exchanges heat by radiation directly with the external ambient. These additional losses were estimated with FEA.

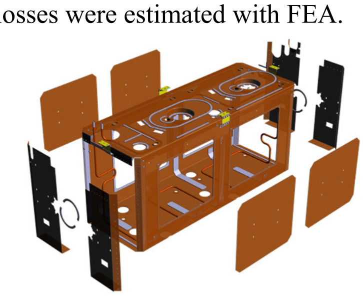

Figure 5: Exploded view of the thermal screen.

FUNDAMENTAL POWER COUPLER

The FPC is one of the main contributor to the losses on the cold mass. It is made of a copper-coated 316LN tube, 3 mm thick, and a warm copper internal antenna. At nominal operation the antenna dissipates 100 W by Joule's effect. This could lead to high temperatures on the antenna, with possible issues of creep, outgassing, and radiation losses to the cold mass. Iterative analyses with HFSS [8] and ANSYS were performed to find the optimal design of the component, which is actively cooled by a room-temperature water flow of 1.5 m·s^{-1} circulating in an internal channel dug in the antenna straight section. The component reaches 100 °C (Figure 6) at the tip of the antenna, and emits heat by radiation towards the cold mass. These losses in dynamic conditions were also estimated with FEA.

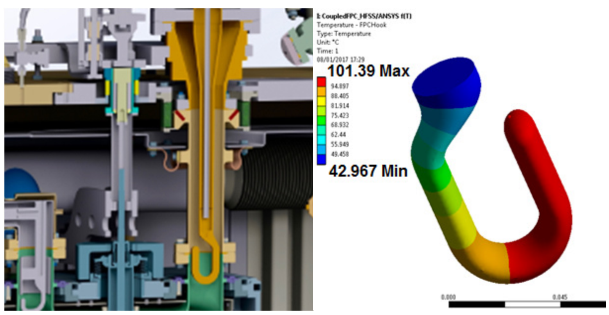

Figure 6: Left: FPC antenna and can. Right: thermal FEA of the tip of the cooled antenna.

The stainless steel tube, is subjected mostly to conduction heat transfer. In this case, however, Eq. (1) can describe only the losses in static conditions. When the RF power is active, additional losses by Joule effect have to be accounted. An analytical solution of the problem is extremely complex, as the electrical resistivity of the component depends on the temperature field and vice versa. A semi-analytical approach was adopted, discretizing the system in several nodes and applying to each node the energy conservation law. The temperature of each discrete element of length *dx* is defined by three equations:

$$Q = -\int_{T_{(x_i-dx/2)}}^{T_{x_i+dx/2}} k(T)\frac{A}{dx}dT$$

$$P_i = \frac{1}{2}\int_{x_i-dx/2}^{x_i+dx/2} I^2(x)\cdot R(x)dX$$

$$I(x) = I_0\cdot 2sin\left(\frac{\omega}{c}x\right)$$

where the index i is referred to the i-th discrete element, T_a and T_b are the temperature at the inlet and outlet of the element, I is the current intensity and R the electrical resistance, P is the power, ω is the wave frequency and c the speed of light in vacuum. As it can be seen in Table 1, the Joule effect generated on the FPC tubes for a nominal duty cycle (P = 40 kW) is relevant, even with a copper coating of the 316LN walls, representing the 25% of the total dynamic losses of the cryomodule.

HOM COUPLERS AND PICKUP

The HOM and pickup lines feature a special design [9] with thin coaxial stainless steel tubes, copper coated (Figure 7). Commercial coaxial cables were also investigated, but the power loss at the duty cycle (1 kW on each) would provoke melting of the cable in operation. The calculation of the heat load to the cold mass in static and dynamic conditions was performed semi-analytically, with the method detailed in the previous section.

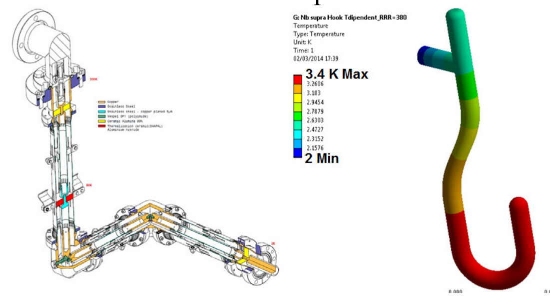

Figure 7: Left: HOM coaxial lines. Right: HOM antenna.

The HOM antenna is in superconducting niobium, as initial simulations showed that the losses on a copper component would be too high. The maximum temperature on the antenna without cooling is 3.4 K. As the niobium critical temperature is 9.2 K, this presents enough margin against quench, with negligible losses to the cold mass (see Figure 7, FEA performed on the preliminary version of the antenna). As an additional precaution, the antenna is cooled with superfluid helium. The pickup antenna, which is less loaded, does not require active cooling. For each line, additional 0.4 W of dynamic losses were included in the estimation, to account for a 50 µm shape tolerance.

BEAM AND CAVITY LOSSES

The beam passage inside the cavities generates surface losses due to resistive-wall impedance. These losses have been estimated to be 0.5 W based on previous experience on superconductive cavities at CERN [10]. The thermal losses on the cavity in operation depend on the thermal efficiency, expressed by the Q factor, degrading at increasing gradients. Recent crab cavity cold tests conducted at CERN for the SPS cavities showed a power loss of about 5 W/cavity at the nominal gradient of 3.4 MV [11]. In the estimation of the total heat budget, 5.5 W per cavity were assumed, to keep into account possible deviations in operation with respect to the measured values.

CONCLUSIONS

The thermal performance of the SPS crab cavity cryomodule was optimized intervening on the design of the cooling circuits and the elements connected to the cold mass or radiating towards it. The design solutions detailed in this paper are the best compromise between the thermal and mechanical requirements of the different components, minimising the heat loss to the cold mass without endangering the structural resistance. The developed analytical and numerical calculation methods were also discussed.

ISBN 978-3-95450-182-3

REFERENCES

[1] G. Apollinari, I. Béjar Alonso, O. Brüning, M. Lamont, L. Rossi, "High-Luminosity Large Hadron Collider (HL-LHC): Preliminary Design Report", CERN, Geneva, Switzerland, Rep. CERN CERN-2015-005, 2015.

[2] F. Carra *et al*., "Crab cavity and cryomodule development for HL-LHC", in *Proc. SRF2015*, Whistler, BC, Canada, 2015, pp. 1160-1466.

[3] C. Zanoni *et al*., "The crab cavities cryomodule for SPS test, presented at IPAC'17, Copenhagen, Denmark, 2017, paper MOPVA096, this conference.

[4] C. Zanoni *et al.*, "Design of dressed crab cavities for the HL-LHC upgrade", in *Proc. SRF2015*, Whistler, Canada, 2015, pp. 1284-1288.

[5] K. Artoos *et al.*, "Development of SRF Cavity Tuners for CERN", in *Proc. SRF2015*, Whistler, Canada, 2015, pp. 1247-1251.

[6] N. Templeton *et al.*, "Design of the Thermal and magnetic Shielding for the LHC High Luminosity Crab Cavity Upgrade", in *Proc. SRF2015*, Whistler, Canada, 2015, pp. 852-856.

[7] V. Parma, "Cryostat design", Lecture at CERN Accelerator School, Erice, Italy, 2013, `https://indico.cern.ch/event/194284/contributions/1472773/attachments/281469/393535/Cryostat_design.pdf`

[8] S. Verdú-Andrés *et al.*, "Thermal Losses in Couplers and Ports of a SPS Double-Quarter Wave Crab Cavity", in *Proc. SRF2015*, Whistler, Canada, 2015, pp. 1219-1221.

[9] C. Zanoni *et al.*, "Engineering Design and Prototype Fabrication of HOM Couplers for HL-LHC Crab Cavities", in *Proc. SRF2015*, Whistler, Canada, 2015, pp. 1279-1283.

[10] O. Capatina, private communication, CERN, 2013.

[11] A. Castilla Loeza *et al*., "CERN cavity results", International review of the crab cavity performance for HiLumi, CERN, 2017, `https://indico.cern.ch/event/590988/contributions/2489635/`